Environmental Sciences Europe

RESEARCH

Open Access

The first spatio-temporal study of the microplastics and meso–macroplastics transport in the Romanian Danube

Ionut Procop[1,8], Madalina Calmuc[2*], Sebastian Pessenlehner[3], Cristina Trifu[4], Alina Cantaragiu Ceoromila[5], Valentina Andreea Calmuc[2], Catalin Fetecău[6], Catalina Iticescu[2,7], Viorica Musat[1*] and Marcel Liedermann[3]

Abstract

Background Transport, accumulation, and degradation of microplastics (MiPs) in the aquatic environment represent a significant concern to the researchers and policy-makers, due to the detrimental impact on biota and human health through food ingestion. Although consistent investigations and research data are available worldwide, comparing the results is still challenging due to the need for more regulations regarding the sampling methods, analysis, and results reporting. The European regulatory efforts include studies on the MiPs transport in the western basin of the Danube River developed with active nets-based multipoint sampling methods from suspended sediments and proposed for standardization. In this context, the present study aimed to address for the first time the transport of MiPs in the Romanian sector of the Danube, starting after entering the country (Moldova Veche) and before the formation of the Danube Delta (Isaccea).

Results The multipoint nets sampling procedure facilitated the collection of suspended sediments in the water columns as deep as 0.0–0.6 and 3.0–3.6 m depths and near riverbed sediments (autumn 2022 sampling) during an extensive spatio-temporal study from spring 2022 until spring 2023. The estimate of the maximum annual transport of 46–51 and 93–100 $t{\cdot}y^{-1}$ for MiPs and total (micro–meso–macroplastics) MPs at Moldova Veche was based on 135 collected and processed samples using 2021 water flow data. Polyethylene (58–69%) and polypropylene (21–33%) were the main polymer components in the separated fragments, foils, microfibers, and different colors spheroids of MiPs (< 5 mm), and the foils and fibers of meso–macroplastics (5–100 mm). Advanced investigations highlighted various microstructural degradations of the plastic fragments at the micro- and nanoscale and attached minerals (clays) and heavy metals.

Conclusion This paper presents the first comprehensive data set for microplastic annual transport in the "Low Danube", filling the need for a complete transport assessment in one of the most significant European rivers. 4–5 times lower values were measured before the entrance to the Danube Delta than those from Moldova Veche. The investigations should continue, including flooding events, and the sampling points should be expanded to deeper water column layers during all the campaigns for further validation.

*Correspondence:
Madalina Calmuc
madalina.calmuc@ugal.ro
Viorica Musat
viorica.musat@ugal.ro
Full list of author information is available at the end of the article

Highlights

1. The first comprehensive data set for microplastic transport in the Romanian Danube.
2. Polyethylene and polypropylene are the main polymer components of the separated plastics.
3. Maximum annual transport of 46-51 and 93-100 t·y-1 for MiPs and total plastics, respectively.
4. 4-5 times lower transport values near the entrance to the Danube Delta than close to country entering.
5. The investigations should continue for further validation.

Keywords Microplastics, Meso–macroplastics, Polymer composition, Plastics morphology, Annual transport yield

Graphical Abstract

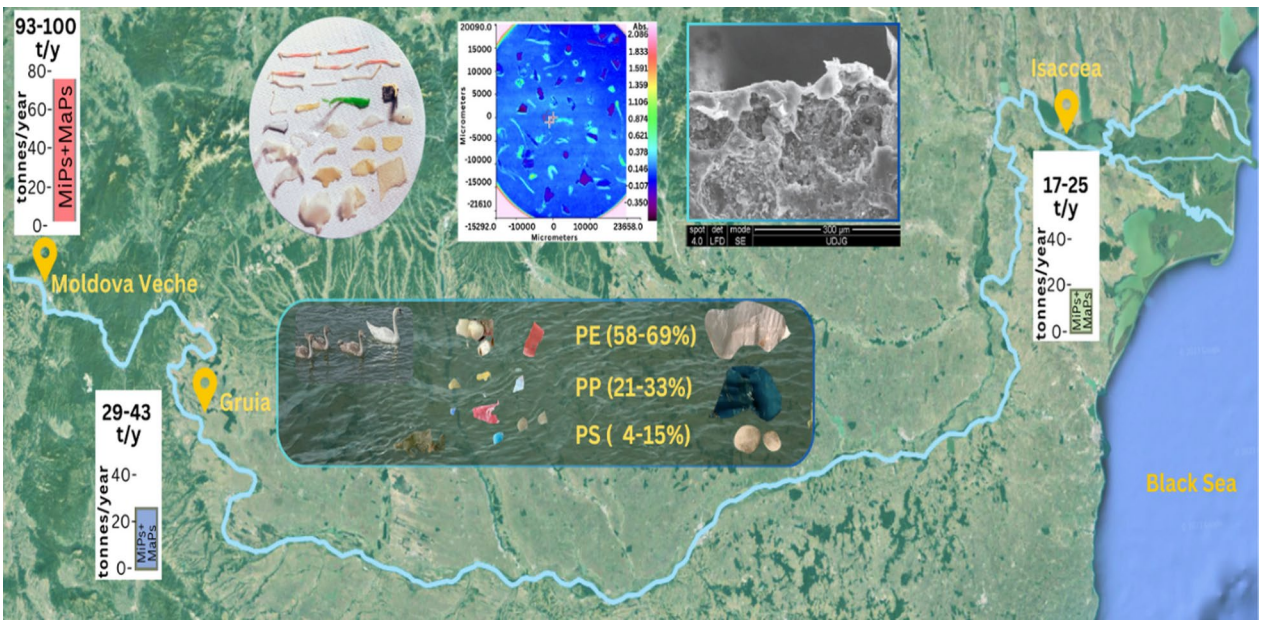

Background

Worldwide plastic pollution has been reported in seas and freshwater courses [1–4], representing one of the biggest pollution problems of the twenty-first century. An alarming increase in the concentration of microplastic pollutants was reported in waters and aquatic environments [5–8]. The terminology "Microplastic," introduced in 2004 by Thompson et al., emerged from the discovery of plastic fragments sized around 20 microns in aquatic sediments collected from UK beaches and seas [4]. In 2009, Barnes et al. proposed the first size-based classification of plastic (synthetic polymers) debris from aquatic environments into four classes: MegaPlastics (≥100 mm), MacroPlastics (MaPs 20–100 mm), MesoPlastics (5–20 mm), and MicroPlastics (MiPs, "larger MiPs" 1–5 mm and "smaller MiPs" 1 µm–1 mm) [9, 10], Later, the classification included the nanoplastic class (NPs, 1 nm < 1 µm) [3, 11]. Microplastic pollutants are divided into two sub-classes: primary microplastics (released directly into the environment from industrial activities: cosmetics, pellets for plastic and composite objects production, paints, fabrics) and secondary microplastics (degradation products of larger plastic fragments under the influence of environmental factors) [5, 6, 8, 9, 12, 13].

There is consistent evidence showing the significant impact of the accumulation and the persistence of MiPs in the environmental factors, plants, and living bodies [14–16]. A scientific paper announcing albatrosses with ingested microplastic dates back to 1969 [17]. Studies since 1980 focusing on the quantity of discarded marine waste following fishing activities highlighted the presence of plastic litter on the remote beaches of Alaska [18]. Plastics that reach the environment gradually degrade

into smaller particles to submicron and nanometer sizes. These particles become fixing agents for bacteria and other contaminants, producing critical toxic environmental effects [15, 19–21]. Mistaken as food and entering the food chain through ingestion, the contaminated MiPs produce inflammatory processes and oxidative stress, in addition to wounds and malnutrition due to the absence of nutritional value, thus endangering the health and development of living organisms (biota) [9]. Both low-density and high-density MiPs particles accumulate on the top biofouling layer and sink into the waterbed sediments, respectively [9, 22], increasing the plastic pollution effects.

Research carried out since the 1970s highlighted that the planetary oceans serve as a final sink for terrestrial plastic debris, generating a continuously increasing concern about the pollution with micro- and nanoplastics [10]. Consequently, the investigation of microplastics in the freshwater sources expanded to the global aquatic environment from salted to freshwaters, surface water, and deeper layers column, floating litter, alluvium in suspension and seabed sediments, beaches and riverine environments, shoreline and river–sea interface section, minerals, and biota [4, 9, 23–27].

Rivers with their tributaries are the essential transport pathways (about 80%) of terrestrial plastics from upstream pollution to the aquatic environment [3], with an estimated transport of between 1.15 and 2.41 million $t^{¨}y^{-1}$ of plastic into the seas [25]. If significant MiPs marine pollution emerges from river inputs, the MiPs quantification into the main rivers and the freshwater environment across different continents becomes of strategic environmental interest. In Europe, such studies were carried out in the big rivers, such as Seine, Rhine and Po [24], Elba [28], Rhône and Besós [13]. The Danube River, the second longest (2857 km) river in Europe extending into the territories of nineteen countries with the most international river basin in the world, is considered one of the main polluters of the semi-enclosed Black Sea Basin, with a previously estimated plastic input of 4.2 $t{\cdot}d^{-1}$ [9]. Evaluation of MiPs and other pollutants in the Danube basin and their impact on the Black Sea pollution is an important European issue. Focusing on accumulating valuable information and knowledge and, specifically, creating simulation models for quantifying the monitoring results [29], predicting, and ultimately reducing plastic pollution should be a top and urgent priority [24, 30–32]. Global models already exist for assessing river pollutant inputs in semi-enclosed sea basins aimed at quantifying MiPs transport that emerged from the terrestrial plastic [30]. Aiming at simulating the microplastic river loading, the models focus on predicting the annual export of MiPs to each related marine sub-basin [30]. Studies applying the MARINA model to assess MiPs pollution reduction methods and to guide environmental policies are under evaluation [33].

The first report on plastic transport by Danube waters emerged from studies on fish larvae [26]. During the last decade, several studies applying active net sampling in the water column (mesh size between 300 and 500 µm) approaching the quantification and characterization of the MiPs and total MPs in the Austrian basin of the Danube River, were conducted by Lechner et al. They estimated annual emissions of 1.533 $t{\cdot}y^{-1}$, but also considerable quantities of plastics (4.2 $t{\cdot}d^{-1}$) that can be transported via the Danube River during the flood seasons [26]. A joint microplastics screening was carried out in the water column of an extended European Danube basin on the territory of eight countries, from Germany to Ukraine, using the sedimentation box method to collect suspended particles [13]. MiPs pollutant input of Danube in the western Black Sea sub-basin and their impact on biota were also published by Strokal [33] and D'Hont [9], respectively. Kiefer et al. reported a very recent comparative study conducted with active sampling methods on the presence of MiPs in the Danube Delta surface waters [34, 35]. The applied net-sampling and net-provided cartridge-based sampling methods were operated with 20, 65, and 105 µm mesh size nets. A continuous important increase of the MiPs particle's number-based concentration was observed when the mesh size decreased from 105 µm (46 $p{\cdot}L^{-1}$) to 20 µm (2677 $p{\cdot}L^{-1}$), concluding the impossibility of comparing the results obtained by different sampling. Some of these studies refer to samples collected in several locations on the Romanian territory of the Danube, such as Giurgiu [13] and Isaccea [34].

Regarding the Romanian River Basin of the Danube, recent comprehensive sediment studies extending almost to the entire Romanian length of the Danube, before the Iron Gates, through the Danube Delta to the discharge into the Black Sea and marine coastal waters were conducted by Pojar [35–37]. A first study addressed the abundance and composition of plastic particles in surface waters of the Western Black Sea and in the discharge area of the Danube branches (near the Danube Delta). The results underscore the presence of fiber and fiber clumps (76.1%), foils (12.7%), and fragments (11.1%) of micro- and mesoplastics with an average concentration of 7 particles/m^3 [37]. Sedimentary microplastic concentrations were measured in 38 sites along the river–sea route, from the Romanian continental river to the Danube Delta and the Romanian and Bulgarian regions of the Black Sea coast [36]. The group also investigated the distribution of microplastics into the superficial sedimentary [35].

This paper presents the results of an extensive study carried out between spring 2022 and spring 2023 on the quantitative, compositional, and morphological characterizations of the suspended plastic particles (MiPs and meso-included MaPs fractions) within the alluvium transported by the Danube waters along the territory of Romania, from the entry of the country to the front of the Danube Delta. The sampling was carried out at three key locations: Moldova Veche (km 1048, meaning 23 km after entering the territory of Romania), Gruia (km 851, downstream of the Iron Gates II), and Isaccea (km 100.2 after the confluence with the last two big tributaries, Siret and Prut Rivers, before the Danube Delta) (Fig. 1). The study applied the multipoint measurements sampling procedure proposed by Liedermann et al. [38], operating with two sampling devices at two or three horizontals (water surface, in the middle, and at the bottom of the water column). This is the first comprehensive data set for microplastic transport on the Danube crossing in Romania. The results fill in the gap of essential information regarding the MiPs transport in the "Low Danube" area, necessarily requested for a complete assessment of the transport and accumulation of MiPs in the European river with the most extensive hydrological basin. The study also joins the European efforts to regulate and standardize active sampling nets-based multipoint methods from the suspended sediments in large flowing waters.

Materials, methods, and devices

Sampling locations

The study included five monitoring seasons (spring 2022 to spring 2023) in three locations on the Romanian route of the Danube, i.e., Moldova Veche, Gruia, and Isaccea (Fig. 1). The satellite images with the position of the three locations and the characteristics of the monitored sections are presented in Figure S1 and Table S1 (Supplementary), respectively. Table S1 indicates the referential geographic positions and the absolute altitude of the "0" level gage station (Zo) in the reference system Black Sea Sulina (mMNS). Sampling started at Moldova Veche to estimate the plastic load entering the country. The monitoring section at Isaccea, located downstream the confluence of the last two big tributaries, Siret and Prut Rivers

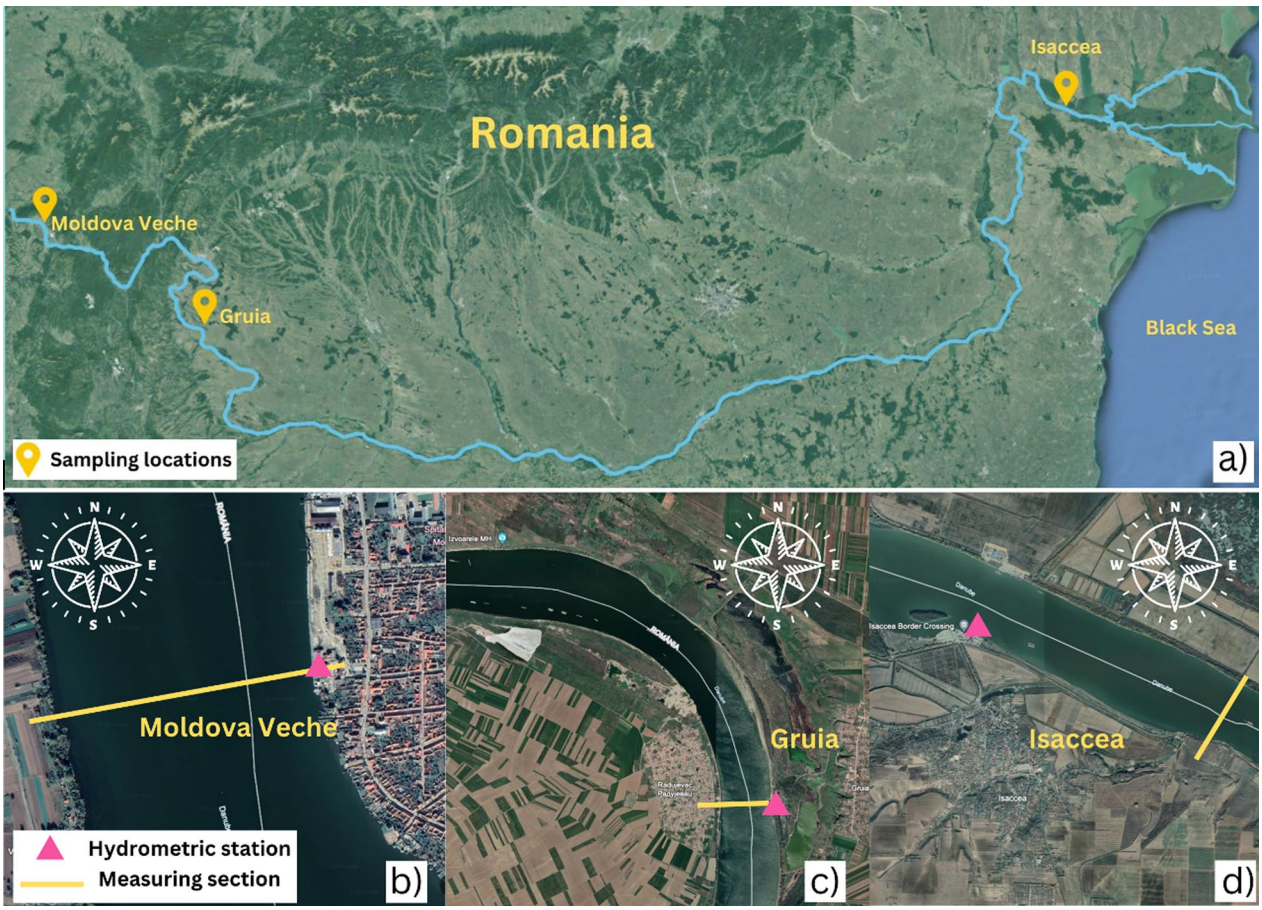

Fig. 1 Overview (**a**) and details for the three sampling locations: Moldova Veche (**b**), Gruia (**c**) and Isaccea (**d**)

and 21 km before the formation of the Danube Delta, was aimed at potential preliminary estimation of the contribution of the Romanian Danube reach the plastic transported by the Danube through the Delta toward the Black Sea.

During the project period, in parallel with the sampling campaigns in the three sections (Moldova Veche, Gruia, and Isaccea), the measurements of liquid flow (Q), water and air temperature (T_{water}, T_{air}), and water turbidity (Table S2) spanned from seven days before sampling and the sampling day for a precise assessment of the hydrometeorological conditions that together with the flow (hydrological regime) may influence the water quality. Table 1 presents the average values measured on the sampling day. The last column represents the mean value of turbidity per section. The liquid flow is also presented as the multiannual mean value of the month. In 2022 year, the hydrological regime remains characteristic of low-average waters. Discharges recorded at the Gruia and Isaccea sections are generally below the multiannual mean value of the month (Q_{mma}), calculated for the period 1984–2020 and presented in Table 1. At the Isaccea section, the discharges show a downward tendency and remain slightly below the multiannual average of the month, calculated for the period 1984–2020 ($Q_{mma} = 8956\ m^3 \cdot s^{-1}$, April 2022).

Monitoring plastic particles consisted of sampling the alluvial materials in suspended sediments, laboratory processing of the collected samples to extract the biogenic materials-free plastic particles, and the qualitative (polymer composition and morphology) characterization and quantification of the extracted MiPs and meso-included MaPs [4].

Sampling methodology and devices

Generally, depending on the specificity of the sampling site and technical conditions available to the user, five groups of sampling methods with specific advantages/disadvantages can be applied (plastic tracking, active sampling, passive sampling, visual observations, and citizen science) [22, 35]. Active methods, such as nets-based sampling, water pumping, and water grabbing, are usually used for plastic sampling in suspended sediments [22].

In this study, the monitoring and the quantification of plastic transport were conducted based on the methodology developed by Liedermann et al. [38] for multipoint sampling of materials in suspension in large rivers. This sampling method utilized benthic nets (100–500 µm mesh size)-based collecting systems anchored to bridges or boats operating with cranes or manta trawl and is proposed for standardization [38]. The used methodology allowed for spatial variability in monitoring the MPs transport in different cross sections (locations) selected along the river for the final estimation of MPs annual transport. The method facilitated accurate multipoint monitoring of the entire section of the river, ensuring flexible measurements at the selected locations across the river. In each section, the sampling was conducted in several vertical profiles at different depths, from the surface until close to the riverbed (only in autumn 2022). This strategy enables the estimation of MPs separately at

Table 1 Hydrometeorological parameters during the sampling day of each campaign (season)

Season	Location	Campaign date	No. of samples	Flow rate/Q_{mma} ($m^3 \cdot s^{-1}$)	Temperature (° C)		Turbidity ($mg \cdot l^{-1}$)
					$T_{(water)}$	$T_{(air)}$	
S1 Spring 2022*	Moldova Veche	24.05.2022	9	4136	21.0	18.5	27.0
	Isaccea	04.05.2022	9	5940/8560	15.3	14.3	61.6
S2 Summer 2022	Moldova Veche	08.07.2022	9	3095	27.3	190	24.9
	Gruia	03.08.2022	9	1860/3847	27.5	25.5	13.0
	Isaccea	20.07.2022	9	3260/6212	27.4	24.4	31.3
S3 Autumn 2022	Moldova Veche	28.09.2022	12	4316	18.3	16.5	34.3
	Gruia	05.10.2022	12	4030/3819	18.5	14.5	30.2
	Isaccea	03.10.2022	12	4737/4615	20.0	12.7	87.0
S4 Winter 2022	Moldova Veche	24.11.2022	9	5509	10.8	5.5	43.0
	Gruia	14.12.2022	9	4874/4928	6.0	0.0	41.0
	Isaccea	08.12.2022	9	5360/5750	9.4	6.2	47.4
S5 Spring 2023	Moldova Veche	16.03.2023	9	7742	7.8	4.0	62.4
	Gruia	05.04.2023	9	6190/7487	10.0	3.0	50.0
	Isaccea	25.04.2023	9	8640/8956	12.8	12.6	62.3

* The first project plan included only Moldova Veche and Isaccea sampling locations but starting from the summer 2022 (S2) campaign, the third monitoring location was introduced at Gruia, to provide information on the effect of the Iron Gates Dams

different water levels but also as average concentrations in the monitored cross sections. The temporal variability was realized by collecting samples at different flow rates during at least one year of consecutive seasons.

Two dedicated devices with two- and three-level sampling, respectively, provided the sampling collections. The two-level device was designed and manufactured in collaboration with UDJG (Fig. 2a, b), inspired by the device developed atpace2022 BOKU for collecting solid alluvial samples from flowing waters [38]. This device is equipped with three capture nets of 3 m in length, fitted in metal frames with an opening size of 0.60 × 0.60 m.

To be aligned with international standards and avoid quick clogging, the size of the net mesh was decided to be 250 µm. Containers with a diameter of 10 cm for collecting samples were placed at the end of the nets (details in Fig. 2b). This alluvial collector was tuned to reach the optimal weight and geometry for controllable hydrodynamic properties in the water flow of the river, which resulted in the most precise positioning of the collection nets at the measuring points (vertically and horizontally). Two anchoring eyes added to the metal frame brought better device stability in the water. Additionally, floats located on each side of the metal frame increased the stability of the device in the water during strong currents. Each net opening was equipped with a flowmeter-type device for measuring the volume of water passing through the respective net during the sampling (detail Fig. 2c). During the autumn season 2022 (S3), the sampling was performed by a three-level device (BOKU) [38].

The sampling methodology in the current study used crane boats anchored on the river. The nets were lowered from the ship's stern into the water and pulled over the side (Fig. 2d, e and S1 (Supplementary)). Our approach differs from the strategy used by other similar studies launching the alluvium catchers with nets from fixed positions (from bridges). The objective during each sampling was to ensure as much water passage through the nets as possible to collect a relevant amount of alluvium, including MiPs and meso-included MaPs, under similar conditions. Based on the water flow during sampling in different areas and seasons, the collection period

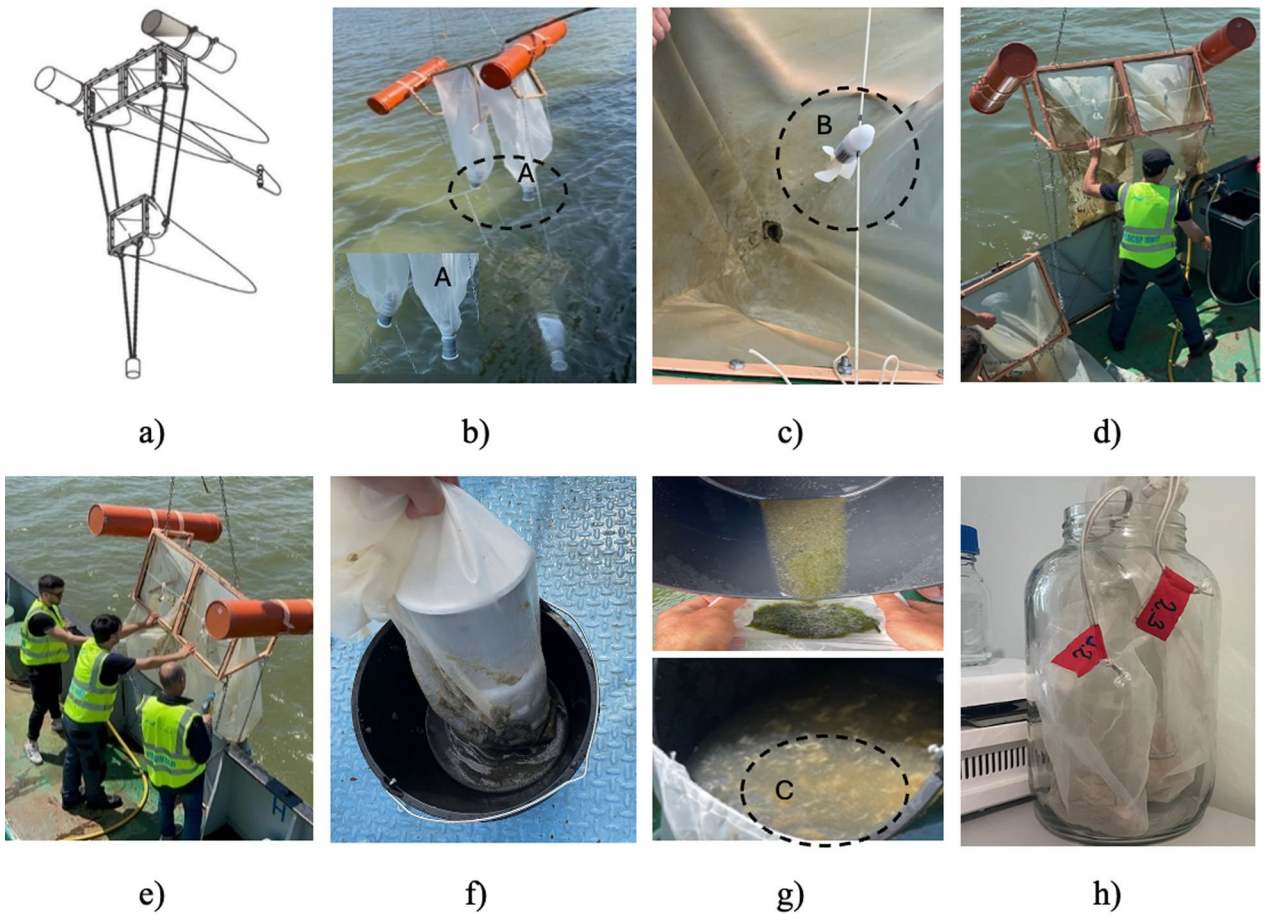

Fig. 2 The two-level sampling device (UDJG device) (**a**–**e**), steps of raw samples preparation (**f**–**g**) and packing (**h**) for sending to the laboratory

spanned between 30 min in extreme discharge conditions and 85 min in normal conditions.

Following the methodology of the reference study, sampling was performed under isokinetic conditions. A mechanical flowmeter (Model 2030R w/3 Dia, supplied by General Oceanics), mounted at the entrance of the water in the collectors, ensured accurate measurement of the water flow filtered through the net. The volume of water (V, m^3) passing through the net, in this study around 1000m^3 of water was filtered in each net, was calculated according to the formula:

$$V = \left\{3.14 \cdot \textit{net opening radius}^2\right\} \cdot d \quad (1)$$

The net opening radius is 0.30 m and *d* is the length of the water column that passed through the net during the alluvium sampling period, which was calculated based on the number of rotations indicated by the device for the sampling period and the device constant. The sampling depths and the distances of the sampling points relative to the Romania shore allowed for the final calculation.

Three (Figure S1 a-c) and four (Figure S1 d) vertical profiles were selected to be monitored using the UDJG device (Fig. 2) during S1–S2 and S4–S5 seasons, and BOKU device during S3 season, respectively. The labeling of the samples according to the sampling experimental conditions is presented in Table S3.

During each campaign, three samples were collected on each vertical profile, totalling nine samples per section. In the spring 2022 campaign (S1), only two sections (Moldova Veche and Isaccea) were monitored, meaning 18 samples. Starting in the summer of 2022, a third monitoring location was introduced at Gruia (Table S3). During season S3 (autumn 2022), the sampling was conducted with the three-level BOKU device on four vertical profiles. In this case, the three water levels (one sampling net for each level) were located at 0.0–0.6 m, the middle (3.5–8.0 m) and near the bottom (6.5–11.7 m) of the water column (Figure S1d), adding up to 36 (12×3) samples for all three monitored stations (Table S3). Therefore, within the five campaigns, 135 samples were collected. These samples were prepared and delivered to the laboratory, where they were processed, quantified (plastic weight), and characterized after separating into two size classes/groups: MiPs (250–5 mm) and meso-included macroplastic MaPs (5–100 mm). The overall plastic resulting from these groups represents the total plastic (MPs) in the present paper.

Preparations for analysis

The preparation of the captured alluvium samples for delivery to the laboratory for processing and separation of MiPs and meso-included MaPs was an important stage and was carefully treated. Thus, by washing with purified water directly in the collection nets, the resulting material was carefully passed into a plastic container (Fig. 1f, g) fabricated from high-density polyethylene (HDPE), a non-reactive thermoplastic suitable for medium to heavy-duty use, resistant to impact, storage, and suitable for transit. From these containers, large objects, vegetation, and megaplastics (larger than 100 mm) were removed after washing under a water jet, ensuring microplastic would not be left on the removed items. The resulting water and the material were poured into sediment filtration bags (175 µm mesh size material). The samples were dried for 48–96 h depending on their size, at ambient temperature. The bags allowed water to drain from the samples and ensured better preservation of the collected sample for the next stage of laboratory processing. The sediment filtration bags were transported to the laboratory into a glass container (Fig. 2h).

Usually, the laboratory processing methods are adapted according to the specifics of the samples and the sampling site environment, but also to the presence of biogenic materials [9, 22]. The laboratory processing of raw samples for separation of the MiPs and meso-included MaPs fragments from the collected materials (Figure S2a) occurred in three steps (Figures S2b–f): digestion of biogenic materials (I), density-based separation of floating plastic fragments (II) and filtering of plastic fragments from the supernatant solution (III). The digestion was conducted in Berzelius glasses at room temperature (Figure S2b) under a 1:1 volume mixture of 10 M KOH and 30 wt.% H_2O_2 solutions (Figure S2c) [37]. Both solutions were gradually and carefully added to the collected alluvial samples, KOH solution being added about 10 min after the hydrogen peroxide. The samples were left to stir for four days, followed by neutralization with formic acid. Samples were covered to prevent contamination during digestion. The separation of plastic fragments from the sediments resulting after digestion is based on changing the solution's density to favor the buoyant plastic (Figure S2d). For this purpose, a 60 wt.% $ZnCl_2$ saturated solution enabled the final solution to reach a density between 1.6 and 1.8 $g.cm^{-3}$ [15]. Finally, the floating plastic fragments were separated from the saturated supernatant solution by filtration under a preliminary vacuum into a separation funnel (Figure S2d-e) and accumulated on filter paper of 47 mm diameter and 2 µm pore size (Figure S2f). After filtering and drying, the resulting plastic fragments were sorted into two size-based groups (Fig. 3): MiPs (250 µm and 5 mm per mesh size) (Fig. 3a) and meso-included MaPs (5–100 mm) (Fig. 3b). These groups were weighed and analyzed in terms of composition, morphology, and quantity.

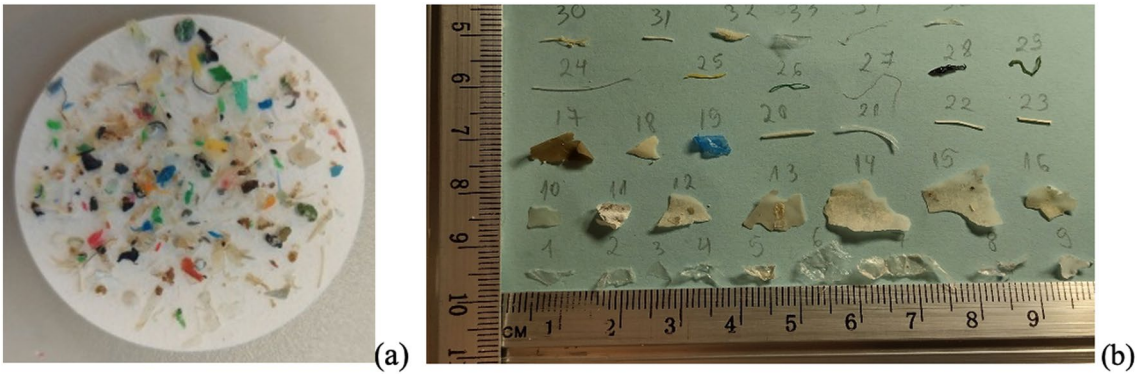

Fig. 3 Digital images of representative MiPs (**a**) and meso-included MaPs (**b**) separated from digested alluvium sample

Figures S4 and S5 (Supplementary) present comprehensive selections of digital images of MiPs and meso-included MaPs samples, respectively, extracted from the collected raw alluvial samples in the three sections during the seasons of the project.

Analysis and calculations

Compositional and morphological analysis of separated plastics

In this study, both collective MiPs samples (Figure S3 in Supplementary) and well-defined individual meso-included MaPs particles (Figure S4 in Supplementary) were subjected to polymer compositional analysis. In the case of meso–macroplastics, the absorption spectrum was recorded in the near-infrared (NIR) range using the FTIR Spectrum3 Fourier-Transform IR Spectrometer (Perkin Elmer, UK) with Attenuated Total Reflection (ATR) on fragments easily visible to the naked eye. The ATR-FTIR parameters used for the analysis of MaPs samples were as follows: 4000–650 cm^{-1} spectral range, resolution of 4 cm^{-1} and 16 scans accumulation. Figure S5 (Supplementary) presents the spectra of the identified polymers based on the comparison with the reference spectra from the equipment database (Polymers S.T. Japan). A minimum match of 90% was considered to identify the polymer. For the simultaneous identification of polymers found in the mixture of the collective MiPs samples (Figure S3 in Supplementary) without separation into individual MiPs segments, a Spotlight 400 micro-FTIR spectrometer (Perkin Elmer, UK) with fluorescence optical imaging in the near IR range was used. The micro-FTIR analysis of MiPs particles was analyzed in 4000 −750 cm^{-1} spectral range at 16 cm^{-1} resolution, 2 scans per pixel, pixel size of 25 µm, and 1 $cm^{¨}s^{-1}$ interferometer speed.

The equipment scanned the entire surface of the collective sample, simultaneously visualizing and recording the optical fluorescent images of the MiPs fragments, sizing the scanned particles, and identifying from FTIR spectra the polymer type in each of the scanned MiPs. Moreover, the particle's thickness is identified by the color of the fluorescence FTIR emission. The morphological study was performed at the macro- and microscopic scales on the individual meso–macroplastic sample. The macromorphologies of micro–meso–macro-fragments were primarily observed by visual analysis of the digital images (resolution 1200 × 1600 pixels) (Figures S3 and S4 in Supplementary). In the case of the collective samples of MiPs left on the filter paper after extracting the meso- to macroplastic fragments, as mentioned before, the micro-FTIR analysis provided supplementary information regarding the number, shape, external size, and thickness of each fragment. Additionally, a Scanning Electron Microscope (SEM) coupled with an Energy-Dispersive X-ray (EDAX) analyser completed our research with more details about size and morphology of the tiny particles and the micro-/nanoscale observation of the surface degradation and chemosorbed species under the influence of environmental and biochemical factors. The microstructures were performed by SEM–EDX system (Quanta 200 model, FEI-Thermo Fisher Scientific, Waltham, MA, USA). The EDX carried out the semi-quantitative concentrations and chemical elements distribution of MiPs on the micro-surface-analyzed samples fixed with a conductive carbon adhesive tape were coated with a thin (8 nm) metal (Au alloy) layer using the Sputter Coater equipment (SPI Supplies, West Chester, PA 19380-4512, USA), to enhance the quality of SEM images. Imagistic results were taken at different resolutions (ranging 1 mm ÷ 10 µm), at an electron accelerating potential of 15 kV.

Calculation methods for plastic quantification

This literature provides a large diversity of microplastic waste presence quantification in the environment, based on both the number of particles [26, 28, 29, 36, 39] and the weight of plastic particles [10], which makes it difficult to compare the results [40]. Our study presents the results of evaluating the transport of the MiPs and total MPs (micro- and meso-included macroplastics fractions) by measuring the quantities of plastic particles with sizes between 250 µm (mesh)-5 mm and 250 µm-100 mm, respectively [4, 16], by gravimetric method [17], after exclusion of larger particles, parts of objects or objects. Each sample containing all the filtered particles was weighed to obtain the total amount of extracted plastic and then sorted into MiPs and meso-included MaPs, followed by separate weighing into the two size classes, using a semi-microanalytical Explorer® Semi-Micro Ohaus EX225DM/AD balance (accuracy 0.01 mg) (Fig. 3).

The quantitative analysis of the resulting plastic materials was carried out following the methodology provided by Liedermann et al. [34, 38], Hohenblum et al. [10] and Pessenlehner et al. (in prep.). In short, several steps for the calculation of the plastic transport in the cross section need to be done:

- **Calculation of the plastic concentration ($g.m^{-3}$)** for each vertical and each net by dividing the captured plastic mass by the filtered water volume.
- **Calculation of the plastic transport rate ($g.m^{-2}.s^{-1}$)** in each sampling point as a product of the calculated plastic concentration with the flow velocity in the sampling point (either taken with an ADCP device or a mechanical flowmeter).
- **Calculation of the mean cross-sectional plastic transport ($g.s^{-1}$; $kg.d^{-1}$)** is then performed by spatial integration comparable to the analysis of suspended sediments as described in [37, 39].
- **Estimation of annual yields ($t.y^{-1}$)** based on several measurements at different discharge conditions can then be determined by the establishment of rating curves and the use of annual flow hydrographs like suspended sediment analysis e.g., described by Haimann et al. [37, 39].

Results and discussion

Polymer composition of plastic samples

The ATR-FTIR spectra of individual meso–macroplastic particles highlighted the presence of polyethylene (PE), polypropylene (PP), polystyrene (PS), ethylene–vinyl-acetate copolymer (EVA), cellulose, polyurethane (PUR), acrylonitrile–butadiene–styrene (ABS), and ethylene–propylene–diene monomer (EPDM) (Figure S5 and Table S4 in Supplementary). The results (Fig. 4) confirmed that PE is the most abundant polymer, representing 57–69% of microparticles, followed by PP with 21% to 33% presence. PS is the third polymer, varying between 4 and 15% in the analyzed collective MiPs samples. EPDM

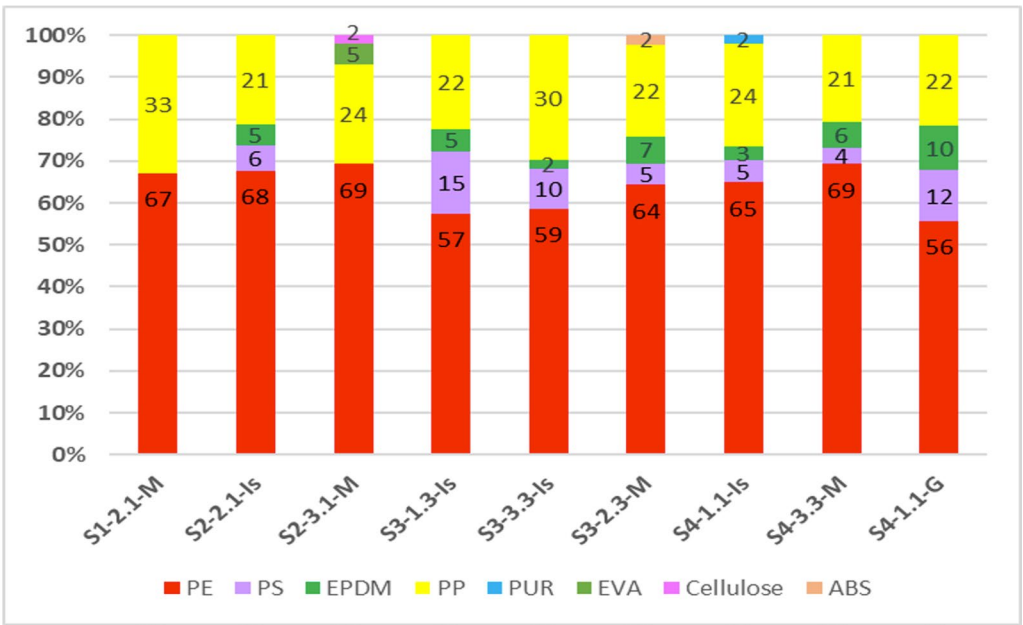

Fig. 4 Polymer composition of the collective MiPs samples in the Moldova Veche, Isaccea stations and Gruia stations, during the spring-winter 2022 seasons

polymer was identified in samples from Moldova Veche (5–7%) Isaccea (3–7%) and Gruia (10%). Additionally, cellulose fibers (2%) were observed in samples taken during the summer season (S2) at Moldova Veche (S2-3.1-M). The spatial variation of the polymer composition can be explained by the presence of riverine pollution sources. Thus, Moldova Veche, Isaccea, and Gruia sampling stations are located near urban agglomerations which may explain the presence of EPDM polymer in the water. This type of polymer is present in the composition of sealing materials used in the construction, engineering, and automotive industries [41]. Regarding the seasonal variation of polymer composition, PE and PP were observed as the dominant ones, in all seasons [42]. However, temporal variations are observed regarding the presence of certain polymers, which can be explained by meteorological conditions (rainfall favoring surface runoff), flow, but also the occurrence of more intense anthropogenic activities in certain seasons. For example, in the summer season (S2-3.1-M), when recreational activities on the watersides are more frequent, cellulose fibers, which are frequently present in the composition of various packaging (Table S5 in Supplementary), were recorded (sample S3-1.3-Is and S3-3.3-Is).

These results are in line with that reported by Pojar et al., highlighting the presence of PE and PP as the most frequently present polymers in the suspended plastics collected with neustonic net (mesh size 200 mm) from surface waters of the Black Sea close to the Romanian shore [37]. Our findings also align with those reported for Danube waters in Romania [13] and the surface waters of the Danube and other rivers in Western Europe [13, 23].

Macro/micromorphology of plastic samples

The morphological classification of plastic fragments refers to foils, three-dimensional polyhedral or acicular fragments, spheroids, and fibers [26]. The visual observation of the digital images presented in Figures S3 and S4 (Supplementary) display all these macromorphologies for the separated plastics from the raw samples collected in the monitored locations during all seasons. Thus, in the 2022 spring season (S1), especially fiber-type meso-included MaPs were collected at Moldova Veche V2 profile surface sampling point specifically (S1-2.1-M), while polygonal fragments and foils predominate in the same profile for deep samples (S1-2.3-M) (Figure S4 in Supplementary). When referring to the corresponding MiPs groups, they are primarily polygonal and spheroidal fragments of different colors, with some microfibers (Figure S3). The samples collected in the summer season (S2) were predominantly in the form of fibers and foils at Moldova Veche and Gruia and large fragments in surface waters at Isaccea (S2-2.1/2-Is) (Figure S4). The autumn season (S3) was rich in micro–meso–macroplastics of different shapes. The S3-2.1-M sample with many microfibers and the S3-2.2-G sample with a complex mixture including polystyrene (PS) granules are noteworthy (Figure S3). In the winter season (S4), the dominant presence of larger follies in Moldova Veche (S4-1.1-M, S4-1.3-M, S4-2.3-M) and Isaccea (S4-3.1-Is) (Figure S4) and the majority presence of PS in Gruia (S4-2.1-G, Figure S3) stand out. The presence of polymer samples with higher (micro)-fiber content can be determined by seasonal variations like the runoff from urban areas, changes in water levels and water flow, but also by specific characteristics of the monitored locations. Thus, in the Moldova Veche area, the riverbed widens and the flow speed decreases. At Gruia area, the "Iron gates" I and II function as a barrier and modify the flow. The accumulation lakes slow down the flow leading to heavier particles to sink [43], favoring the transport of fibers and polystyrene which is less dense and has the tendency to travel longer distances [44, 45]. Very few or no fragments of meso-MaPs were observed in the depth samples collected from Isaccea in the Summer (S2-2.3-Is) and Winter (S4-2.3-Is) seasons (Figure S4). Corresponding samples of MiPs were present as small elongated or polygonal fragments (Figure S3).

The NIR fluorescence images of the MiPs collective samples (Fig. 5) simultaneously provided, in addition to identifying the types of polymers discussed above, morphological information on the shapes, sizes, and thickness of these particles. A general observation revealed a variety of shapes (polyhedral, acicular, and spheroidal, but also several microfibers), sizes between 0.5 and 5 mm, and different colors associated with the thickness of the particles. Upon closer observation, different color variations are found on the same particle, revealing differences in particle thickness. Moreover, different patterns of color variation were observed in Fig. 5, suggesting complex degradation types and levels and/or smaller particles attachment.

Figure 6 shows advanced micromorphological changes on the surface and at the edge of a fragment of MiPs (Fig. 6a) extracted directly from a collected alluvium sample. According to the ATR-FTIR spectrum (Figure S7), the identified polymer of this fragment is polyethylene. The images emphasize complex mechanisms of degradation under the impact of various natural factors, such as UV radiation, waves, dissolved chemical compounds and microorganisms, included into the natural waters. High porosity (Fig. 6b–f) and flake-type fragmentation morphology at micro- and nanoscale (Fig. 6f) were observed, in agreement with the results reported in the literature for PE degradation [46]. Attachments of fragments and fibers up to 10 µm size are also present (Fig. 6b). The EDX analysis completed these results with information

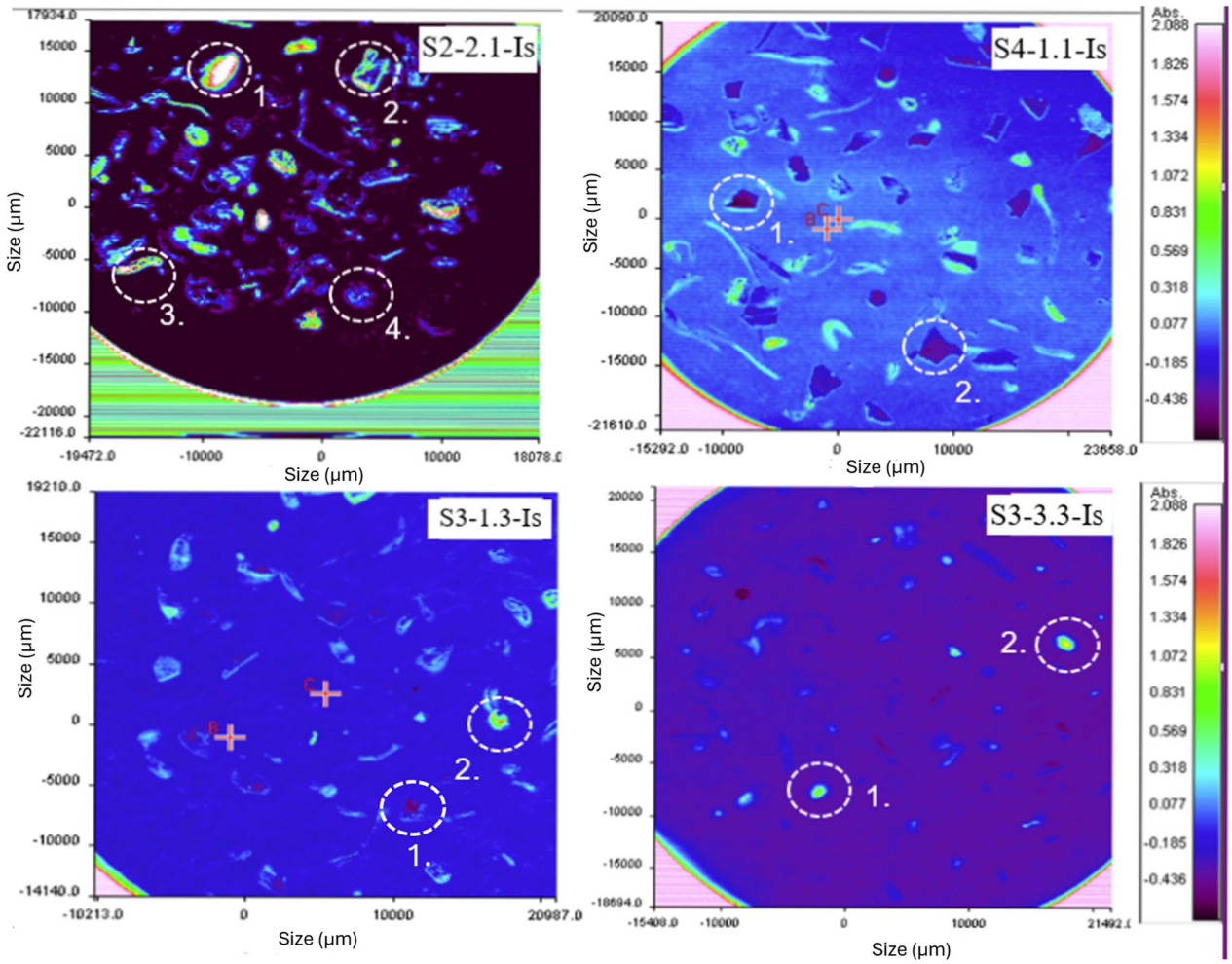

Fig. 5 NIR fluorescence optical images of MiPs collective samples separated from the Isaccea alluvial samples collected in the summer of 2022 (S2-2.1-Is), winter of 2022 (S4-1.1-Is) and autumn of 2022 at shore-surface(S3-1.3-Is) and in channel depth water (S3-3.3-Is). The color scale of the MiPs fragments is proportional to their thickness

regarding the elemental chemical composition at the surface of the analyzed fragment. The SEM–EDX spectra and maps) (Fig. 7) highlighted primarily carbon (95 + wt.%) presence, confirming the organic/polymeric nature of the analyzed sample. The presence of oxygen (~ 10 wt.%), silicon (1.3 wt.% and aluminum (~ 0.3 wt.%) along with elements, such as Fe, Ca, and Mg, but also Ti (~ 0.4 wt. %) in notable quantities indicates the presence of aluminosilicate minerals (clay type). Also, heavy metals like Pb (12 wt.%) and Hg (4 wt.%) are present. It should be noted that both types of components, minerals, and heavy metals, were highlighted on the fragment of MiPs extracted directly from the sample brought to the laboratory (Figures S2 b) and from samples resulting from the digestion of biogenic tissues (Figure S2c). The spatial distribution of these elements (elemental maps) primarily highlights the adsorption of mineral components on the external edges of the analyzed fragment due to the lack of carbon and the presence mainly of Si on its outline. The maps also show agglomerations of Si, Al and O atoms highlighting possible larger mineral particles or major adsorption of minerals on smaller pieces of plastic with a high degree of physical and chemical degradation (Figure S8–S11). Such agglomerations are also present for heavy metals (Hg) (Figure S9).

A comparative analysis of the EDX spectra, distribution of the chemical elements especially for carbon and silicon but also Al, Cu, and Ti (elemental maps in Fig. 7 and Figures S8–S11), superimposed on the corresponding SEM images of the analyzed samples presented in the same figures, clearly shows that the Si-based minerals (clays) have fixed mostly at the edge of the particle, increasing its thickness in the fixing area. The observation is confirmed by the particles' color variation in the NIR fluorescence optical images (Fig. 5). This is the case of particles that appear with blue-green colors at the edge (higher

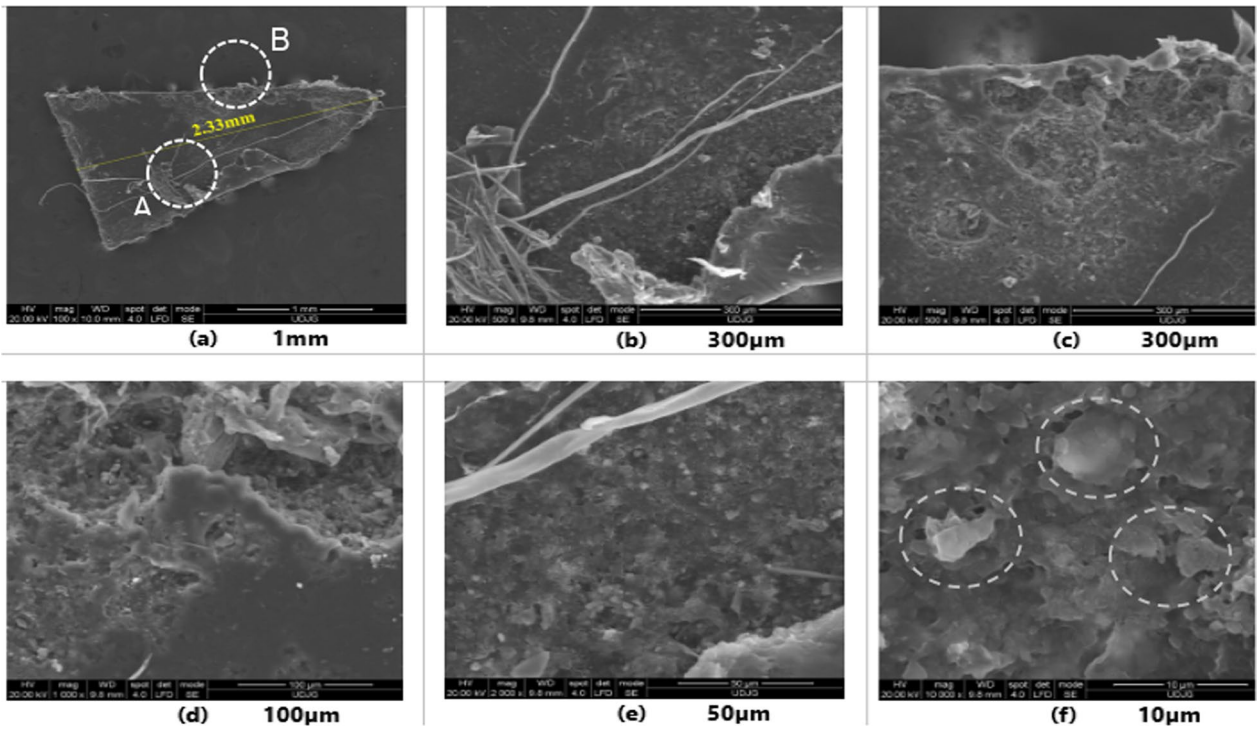

Fig. 6 SEM micrographs of a MiPs fragment (**a**) extracted directly from the collected alluvium sample S4-3.1 G and some details (**b**–**f**). Details from A area (**b**, **e**–**f**) and B area (**c**–**d**)

thickness) and dark-blue purple colors in the middle (less thickness) (details 1 and 2 for sample S4-1.1-Is and detail 2 for sample S2-2.1-Is). Different attachments on the surface of particles are also confirmed in Fig. 5 by a higher thickness of the particle in the middle (green-yellow colors in the center) compared to blue-violet at the edge areas (detail 1 for sample S2-2.1-Is, detail 2 for sample S3-1.3-Is and details 1 and 2 for sample S3-3.3-Is). The detail 1 for sample S3-1.3-Is shows one-color (purple) particle, which means homogenous thickness (small).

The degradation of plastic particles in the natural environment, especially in the aquatic environment, represents a very complex process considering the above-mentioned factors. The contributions of these factors in the global degradation process are different, depending on the specifics and characteristics of sampling sites. Recent studies highlight that the degradation rate is highest on beaches and for floating plastics due to UV exposure, while in sediments, it degrades low to very low [47]. Microorganisms play a crucial role in accelerating the degradation and fragmentation of floating plastics [37, 48, 49].

Supposing the different types of polymers and additives in the plastic materials in which synthetic polymers are embedded are also considered, the complexity of plastic breakdown under natural phenomena highly increases. That is why very few types of polymers have been investigated under the aspect of degradation in the aquatic environment. Thus, studies were reported on the degradation of polyethene in oceans, which proved to be less stable than PP [14, 47, 50]. Currently, studies approaching this subject systematically and comprehensively are limited. The investigation of the macroplastic degradation mechanisms into micro and nanoplastic fragments is of high interest and requires special attention in the context of reducing micro-/nanoplastic pollution in the ecosystem.

Quantitative analysis of separated plastics

Single point concentration

Figure 8 shows the seasonal variation of the sampling point concentration of micro- and total plastics for samples collected at the V1 and V2 profiles, corresponding to the shore and central river sites, respectively, at two levels (0.0–0.6 and 3.0–5.6 m depth).

Regarding the temporal variations, a first general analysis shows that during the Spring 2022 (S1) and summer 2022 (S2) seasons, characterized by low precipitation (Table 1), lower amounts of MiPs and total MPs were recorded, compared to those from autumn (S3), winter 2022 (S4) and spring 2023 seasons rich in precipitations. An exception is the total MPs sample collected in Moldova from the channel area (V2 profile) in-depth water in

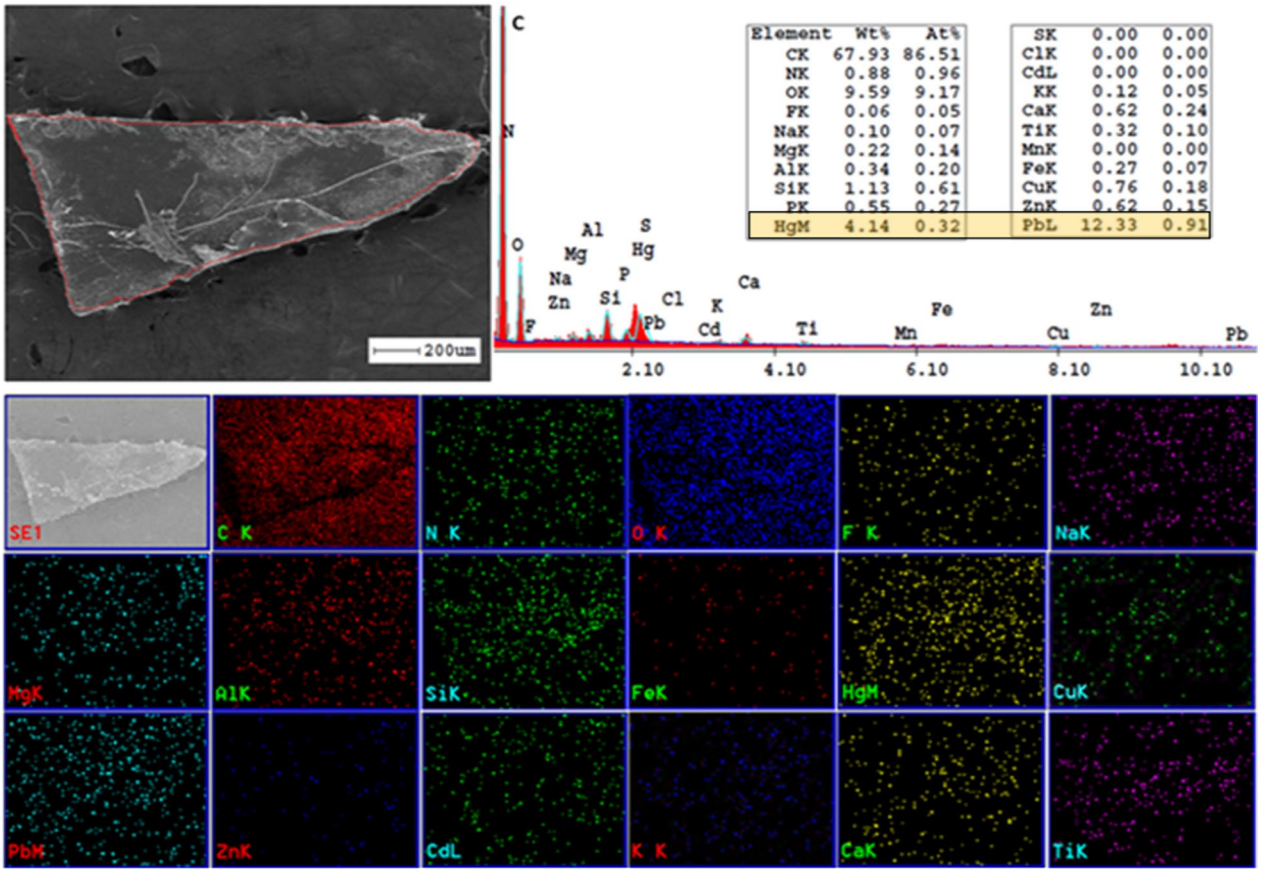

Fig. 7 EDX analysis of MiPs fragment (corresponding to Fig. 6a) extracted directly from the collected alluvium undigested sample (S4-3.1 G): electron secondary image of MiPs (upper left side) (20 µm scale bar); EDX spectrum and semi-quantitative results of identified elements (upper right side) and chemical elements distribution on the surface (bottom side)

the spring 2022 first campaign (Fig. 8h). The spatial variation by location, generally shows that the samples collected in Moldova Veche contain amounts of MiPs and total MPs of 3–5 times higher than those from Gruia and Isaccea. Important exceptions to this trend are the total MPs at Isaccea in the spring of 2023 (S5) at the shore-surface water (Fig. 8b) and the MiPs and total MPs samples collected at Gruia in the S3 season from the channel area-deep water (Fig. 8g, h). For Isaccea, the high value correlates with the highest flow rate in the spring of 2023 (Table 1). Regarding the spatial distribution in the water column and the monitored profiles, similar trends can be observed for both shore and channel areas. Thus, on the surface (Fig. 8a–b, e–f), larger quantities of plastics were observed compared to the deep layer (Fig. 8c–d, e–f), especially for shore areas (Fig. 8a, b). For example, during the collection from winter 2022 (S4 season) in the near-shore area at Moldova Veche, very important amounts of MiPs (Fig. 8a) and total MPs (Fig. 8b) were registered. The MiPs concentration was so high, necessitating additional recovery/extraction steps from the sediment through redispersion in distilled water, centrifugation, and filtration. Four MiPs fragments from this sample (Figure S6) were investigated by ATR-FTIR and SEM–EDX (Figure S11). The FTIR spectra identified three polymers, namely PE, the PE-PP copolymer, and EPDM. A detailed SEM–EDX analysis highlighted areas with Cu, Zn and Hg (6.6 wt. %) and Pb (17.4 wt. %) heavy metals. It should be noted also that for this location, the amount of MiPs in the channel profile surface water (Fig. 8e) is also the highest in this season (S4) compared to all stations, suggesting a massive pollution in a wide area of the river, from shore to the channel. We mention here again the extremely large amount of MPs collected at Isaccea in the spring of 2023 (S5) at the shore-surface water (Fig. 8b). As a general observation, the concentrations of MiPs and MPs remain high also in the depth layers (3.0–3.6 m) from both profiles (V1–V2), indicating agglomeration and fixation on minerals, flora, and fauna, which is crucial for the aquatic environment's biosphere [10].

Total MPs fragments observed in Moldova Veche in spring 2023 are due to a direct increase of water

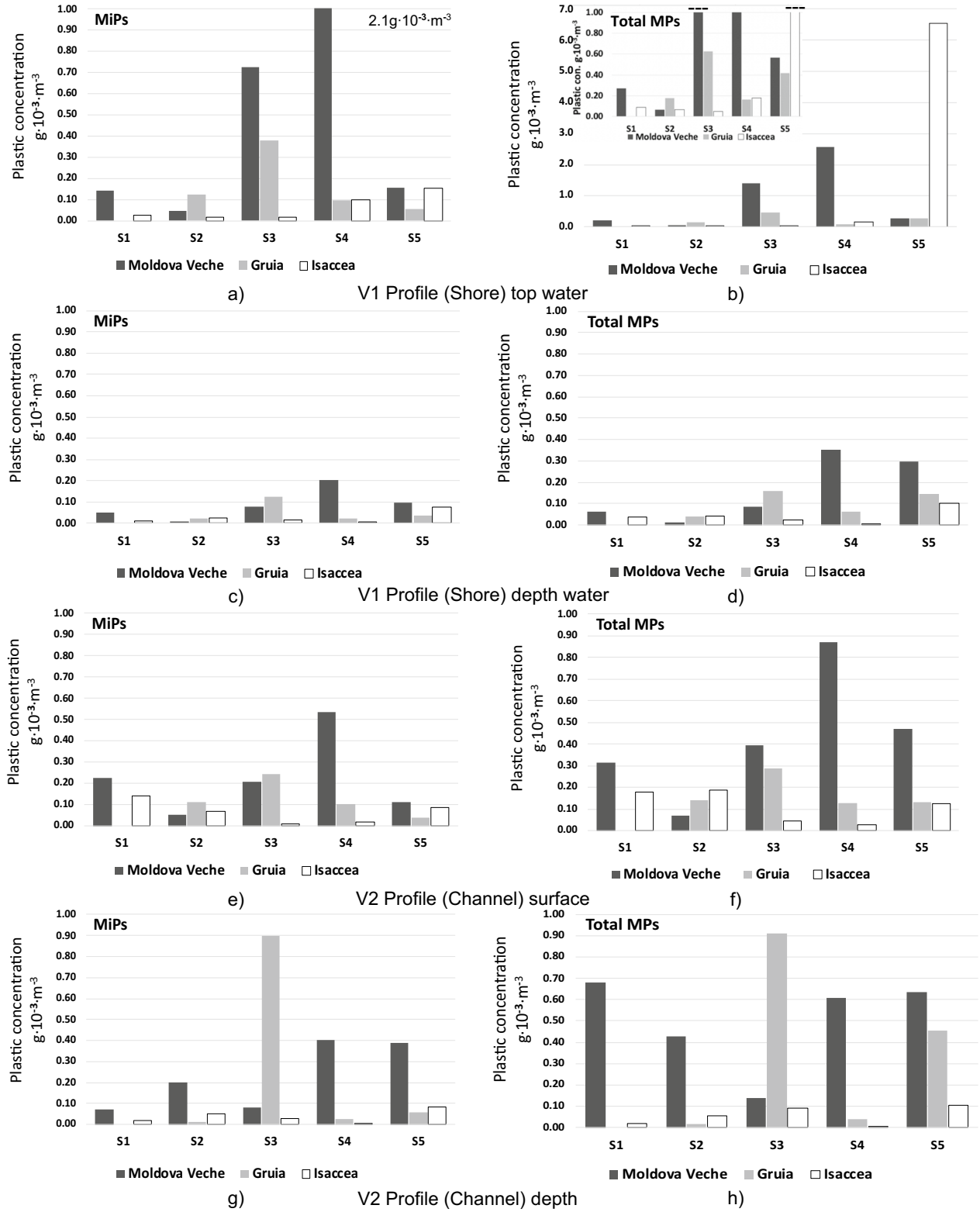

Fig. 8 Seasonal variation of the sampling point concentration of MiPs (left) total MPs (right) of samples collected on V1 (**a**–**d**) and V2 (**e**–**h**) profiles at surface 0.0–0.6 m (**a**, **b**) and at 3.0–3.6 m depth (**c**, **d**) for all the 14 campaigns at the sampling locations. S1-S5 represent the subsequent seasons of the sampling campaigns, from spring 2022 to spring 2023 (Table 1)

discharge. In the spring 2023 collection campaign, the flow rate has the second highest value (after Isaccea) during the entire study (Table 1). This high flow, generated by the melting of the snow together with other precipitations, washed the high plastic quantities from urbanized areas. The observation is also confirmed by a large amount of plastic, especially meso–macroplastic, which was collected in Isaccea, as previously mentioned (Fig. 8d), where the highest flow rate was recorded (Table 1).

Transport of plastics in the sampling sections. First estimation on annual transport in the Romanian Danube

The understanding of the dynamic of microplastic transport in rivers is possible by continuous monitoring of the sediments in suspension and shoreline. Also, understanding the spatial and temporal variables can provide a better assessment of the influencing factors [47]. The Danube River represents a complex environment, and the transport of particles is influenced by their physical characteristics, processes, such as sedimentation, resuspension, and aggregation, and depends on water column stability and the river flow. Seasonal changes are also important factors that contribute to the river dynamics by the transportation of a higher number of particles from the urban and industrial areas. Another aspect that contributes to the dynamic of plastic particles is human activity like dam's constructions, where microplastics can accumulate and continuously degrade [48].

In this paper, the evaluation of the annual transport of MiPs and MPs was based on the discharge values of both 2022 (a year marked by severe dryness, in which four of the five campaigns took place) and 2021, which exhibited a hydrological behavior closer to "normal". After drying, sorting, and weighing according to the described methodology, the plastic transport of each sampling was calculated at all three monitoring cross sections. Creating the rating curves allows a correlation between water discharge and plastic transport by repeatedly measuring under different hydrological and seasonal conditions and assigning the prevailing flow situation. Since plastic sampling and the analysis of the collected samples are very time-consuming and cost-intensive, especially on large rivers, only a limited number of measurements per stretch were possible within the study. To account for this shortcoming in the evaluation, various mathematical functions (linear, exponential, and potential) were used to extrapolate the functions used to calculate the annual plastic transport yields [38].

Figure 9a exemplifies a single measurement performed at the Gruia location for total plastic. Similar representations were created for each plastic measurement at the monitoring sites, plotted separately for MiPs and total MPs. The single measurements and the resulting rating curves are expressed in daily transport ($kg \cdot d^{-1}$). As seen in Fig. 9a, due to the natural scattering of the data resulting from the individual measurements, there is a significant variation when adjusting certain mathematical functions. However, in this manner, it was possible to estimate the potential range of plastic transport in the Romanian sector of the Danube, as is often done when dealing with limited data. From Fig. 9a, the variation of the determination coefficient (R^2) value indicates better experimental data fitting with the linear model (dashed black line). These results also highlight the effect of the sampling points number and their distribution in the monitored cross-section. In this regard, the blue dot, corresponding to the multi-sampling BOKU experiment during season S3 (autumn 2022), closely approximated the curve for the latter model. This season's experiment accumulated a double number of samples, compared to the other seasons. Thus, 36 samples were collected on four verticals at three levels, from the surface to near the bottom (6.5–11.7 m) of the water column (Figure S1d in Supplementary), at all three monitored stations.

Using the rating curves and the hydrographs of 2021 and 2022, the daily plastic loads were calculated accordingly, and by accumulating them, an annual load of MiPs and total MPs was determined for the three mathematical functions applied. The cumulative transport variation for total MPs at Gruia station is presented in Fig. 9b. Figure 9c–f shows the resulting annual transport values generated using the three mathematical functions. Values for 2021 are depicted in Fig. 9c, d, and those for 2022 in Fig. 9e, f. While the graph shows that using the different mathematical functions only leads to minor deviations in the accumulated annual transport yields, a distinct variation of the transported plastic quantities between the three monitoring sections is evident, both for micro- and total plastic.

Table 2 centralized the results showing the value ranges representing the minimum and maximum values obtained using the three above-mentioned mathematical functions and presented in Fig. 9c–f.

Data in Table 2 reveals that the highest transport yields were observed in Moldova Veche with 46–51 and 93–101 t/y^{-1} for MiPs and total (micro–meso–macro) MPs, respectively, for normal hydrological conditions (2021). Based on the measurements so far, it was found, that the annual transport is significantly lower at Gruia (9–18 (MiPs) and 29–43 (total MPs) $t \cdot y^{-1}$) and Isaccea—before entering the Danube Delta (9–14 (MiPs) and 17–25 (total MPs) $t \cdot y^{-1}$), compared to Moldova Veche in the same year (2021).

In principle, it could have been assumed that the transport of MiPs would increase along the course of the

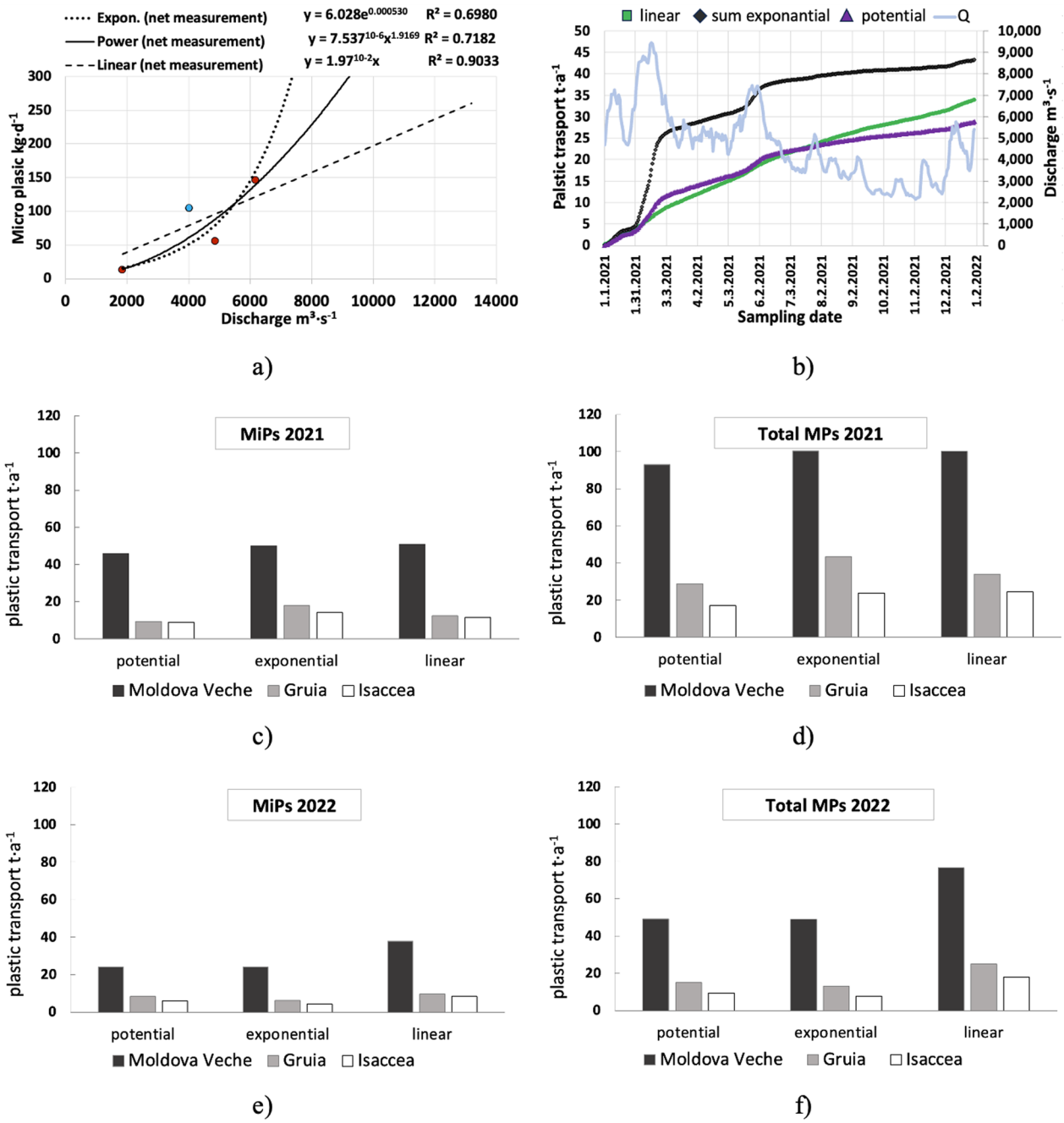

Fig. 9 The rating curve (**a**) and corresponding accumulated annual transport (**b**) assigned to total MPs for samples collected at Gruia station, calculated using three mathematical functions (linear, exponential, and potential) based on the hydrographs for 2021 (**a**, **b**). Cumulative MiPs and total MPs transport in the monitored sections calculated using three mathematical functions (linear, exponential, and potential) based on water flow values from 2021 (**c**, **d**) and 2022 (**e**, **f**). The points in figure (a) express in daily transport (kg·d^{-1}) through the monitored section during monitoring day. The blue dot corresponds to BOKU experiment during autumn 2022. The red dots correspond to GWP Romania-UDJG experiments during summer, winter 2022 and spring 2023 seasons

Danube. The measurements, however, show this is not the case, at least at low to average discharge conditions. Our findings showed lower transport values in the Romanian Danube when compared to those reported earlier for the upstream Danube waters [26, 34], but comparable or a little higher (depending on the water flow of the considered year) with those obtained by Hohenblum et al. (< 17 t¨y^{-1} MiPs and < 41 t¨y^{-1} total MPs) at Hainburg

Table 2 Annual transport yields for the monitored stations

Sampling locations	Cumulated transport yield ($t\,y^{-1}$)			
	2021 water flow		2022 water flow	
	MiPs	Total plastic MPs (MiPs + meso-included MaPs)	MiPs	Total plastic MPs (MiPs + meso-included MaPs)
Moldova Veche	46–51	93–100	24–38	49–76
Gruia	9–18	29–43	8–10	15–25
Isaccea	9–14	17–25	6–8	9–18

[10]. A very recent study (Strokal, M., 2023) reports the estimated of rivers export of macro- and microplastics to seas "by sources worldwide" using MARINA-Plastics model for riverine plastic exports. This study was based on the data of plastic transport in rivers from several continents, for example Weser (1.3 $10^3 t¨y^{-1}$), Elbe (15 $10^3 t¨y^{-1}$), Rhine (0.5–6 $10^3 t¨y^{-1}$), Rhone (0.7 $10^3 t¨y^{-1}$), Danube (3, 550, 1533 $10^3 t¨y^{-1}$), Seine (1100 $10^3 t¨y^{-1}$), Tiber (1721 $10^3 t¨y^{-1}$), Saigon (1100 $10^3 t¨y^{-1}$), Jakarta area (2100 $10^3 t¨y^{-1}$), Motagua (155 $10^3 t¨y^{-1}$), Tiber (1722 $10^3 t¨y^{-1}$), Meycuayan + (13812 $10^3 t¨y^{-1}$). The estimation of rivers export was about 0.5 million $t{\cdot}y^{-1}$ worldwide, of which MiPs are majority into 40% of the basins in Europe, North America, and Oceania (sewage effluents source), MaPs were dominant in African and Asian rivers (mismanaged solid waste source) and in 10% of the basins, macro- and microplastics in seas (as mass) are closed important (high sewage effluents and mismanaged solid waste sources) [49].

Even the present study is comprehensive, it presents just initial data for microplastic transport on the Romanian Danube. For a more in-depth discussion of the processes regarding variance, possible sinks, dependencies on discharge, etc., more measurements are needed (especially for higher discharge situations). The author team is currently working on a manuscript that will comparatively analyze some of the first data sets on the Danube (Pessenlehner et al.).

Conclusions

This spatio-temporal study aimed at bringing forward the first comprehensive data set for microplastic transport in the Romanian sector of the Danube, from close to entering the territory of Romania (Moldova Veche location) until before the Danube Delta formation (Isaccea location). Our findings are based on 135 samples collected during five seasons using active multipoint sampling in three river cross-sections: Moldova Veche, Gruia, and Isaccea.

Polyethylene is the main component (58–69%) in the analyzed samples, followed by polypropylene (21–33%); occasionally, PS, EVA, and EPDMS were also identified. MiPs are polygonal fragments, foils, and spheroids of different colors. In addition, the meso-included MaPs consist of fragments of semi-transparent and/or porous thin or ultrathin foils, fibers, and fibers-clumps, especially for the spring of 2023, the richest in precipitation season during the study.

The environmental-based degradations of plastics in the context of decreasing the dimensions of the persistent and mobile organic pollutants at micro-/nanoscale in the ecohydrosystem is very topical issue. Using advanced NIR fluorescence optical images and SEM–EDX investigations of both digested and non-digested plastic particles (extracted from collected samples), our study showed complex microstructural degradations at the micro- and nanoscale and identified the presence of various (chemo)sorbed components, especially minerals (clays) and heavy metals.

Based on the 2021 water flow, the annual transport estimate was 46–51 and 93–100 $t¨y^{-1}$ for MiPs and total MPs, respectively, at Moldova Veche. The values for Gruia and Isaccea were approximately 4 to 5 times lower. A paper presenting a detailed comparative discussion regarding the transport of MiPs along the European Danube River, from upper to lower sectors, is in progress (Pessenlehner et al.).

The obtained results fill in the lack of information regarding the MiPs transport in the "Low Danube" area, which is essential for a complete assessment of the transport and accumulation of MiPs in the European river with the most extensive hydrological basin. The study also joins the European efforts to regulate and standardize active sampling nets-based multipoint methods from the suspended sediments of flowing large waters.

The investigations should continue, including flooding events, and the sampling points should be expanded to deeper water column layers during all the campaigns for further validation.

Abbreviations

MiPs	Microplastics
MaPs	Macroplastics
MPs	Total microplastics
ATR-FTIR	Attenuated Total Reflection Fourier-Transform InfraRed Spectrometry with
(micro-)FTIR	(Micro)Fourier-transform infrared spectroscopy
NIR fluorescence	Near-infrared fluorescence
SEM	Scanning electron microscopy
EDAX	Energy-dispersive X-ray analysis
PE	Polyethylene
PP	Polypropylene
PS	Polystyrene
EVA	Ethylene–vinyl-acetate copolymer
PUR	Polyurethane
ABS	Acrylonitrile–butadiene–styrene
EPDM	Ethylene–propylene–diene monomer

Supplementary Information

The online version contains supplementary material available at https://doi.org/10.1186/s12302-024-00969-8.

Supplementary material 1: Figure S1. The profiles of the monitored sections from the three locations: Moldova Veche (M), Gruia (G) and Isaccea (Is); Figure S2. Illustration of the experimental steps for the separation of MiPs and meso-MaPs fragments from the alluvium samples: collected dried alluvium samples (a-b), digestion of biogenic materials (c), separation of plastic material on the top of supernatant solution (d-e) and filtering of plastic fragments (e); Figure S3. Selection of digital images of the collective samples of MiPs left on the filter paper after the extraction of the meso-MaPs fragments; Figure S4. Digital images of the meso-included MaPs fragments separated from the alluvium samples collected during the S1-S4 2022 seasons in the three monitored locations, after digestion of the biogenic materials; Figure S4. ATR-FTIR spectra of the meso-included MaPs fragments separated from digested samples collected from Moldova Veche and Isaccea; Figure S6. Identification of the polymer composition for the extracted fragments from the separated MiPs fraction after the digestion of the sample collected at Moldova Veche in autumn 2022 (S4)-shore-surface (S4-1.2-M); Figure S7. ATR-FTIR spectra of a non-digested MiPs fragment from the sample collected at Gruia in the Spring 2023 season; Figure S8. EDX analysis of MiPs fragment detail (corresponding to Figure 6b) extracted directly from the collected alluvium sample S4-3.1-G (before digestion): electron secondary image of MiPs (a) (50 µm scale bar); EDX spectrum and semi-quantitative results of identified elements (b) and chemical elements distribution on the surface (c); Figure S9. EDX analysis of MiPs fragment detail (corresponding to Figure 6d) extracted directly from the collected alluvium sample S4-3.1-G (undigested): electron secondary image of MiPs (a) (20 µm scale bar); EDX spectrum and semi-quantitative results of identified elements (b) and chemical elements distribution on the surface (c); Figure S10. EDX analysis of MiPs fragment detail (corresponding to Figure 6f) extracted directly from the collected alluvium sample S4-3.1-G (undigested): electron secondary image of MiPs (a) (2 µm scale bar); EDX spectrum and semi-quantitative results of identified elements (b) and chemical elements distribution on the surface (c); Figure S11. SEM image on the surface of digested MiP fragment "2" (Figure S7) identified as EPDM polymer in S4-1.2-M sample (upper left side (A)) (200 µm scale bar); EDX spectrum and semi-quantitative results of identified elements (upper right side); chemical elements distribution on the surface (bottom left side (B)) and similar results for a detailed (20 µm scale bar) area (B). Table S1. The referential geographical positions of the monitored sampling sites on the Romanian sector of the Danube; Table S2. Experimental procedure for measurement of the hydrometeorological parameters, Table S3. Labeling of the samples according to the experimental sampling data, Table S4. Identified polymers based on the ATR-FTIR spectra of individual meso-included MaPs fragments; Table S5. Sampling point concentration of MiPs and total MPs samples in two monitored vertical profiles (V1 and V2).

Acknowledgements

The study presented in this paper was carried-out by the project "Dunărea la Raport/Reporting on Danube" implemented by Parteneriatul Global al Apei din România—GWP-Romania and "Mai Mult Verde" NGO associations, within the framework of "Cu Apele Curate"/"Clean Waters" program, supported by Lidl Romania. All these parties are greatly acknowledged. Dr. Martin Hinterleitner is acknowledged for contributing to the measurement team during S3 sampling season (autumn 2022). Director Dr. Eng. Angela Stela Ivan (Galati Lower Danube River Administration) and Dr. Eng. Ioan Mateescu (ROMEXIM SRL București) are acknowledged for key contributions in providing the logistic support during the sampling of suspended alluvium and the selection of the sampling locations on the Romanian sector of the Danube, respectively.

Author contributions

I. Procop: conceptualization, methodology, investigation, writing-original draft, writing-review & editing, visualization, project administration, funding acquisition; M. Calmuc: methodology, investigation, writing-original draft, visualization; S. Pessenlehner: conceptualization, methodology, validation, formal analysis, writing-review & editing; C. Trifu: resources, investigation, manuscript revision; A. Cantaragiu Ceoromila: resources, investigation; V. A. Calmuc: investigation; C. Fetecău: methodology, resources, validation (design, manufacture and testing of the udjg sampling device in the testing basin of UDJG); Cătălina Iticescu: resources, visualization, supervision, funding acquisition; V. Musat: conceptualization, methodology, writing—original draft, writing-review & editing, visualization, supervision; M. Liedermann: conceptualization, writing-review & editing. All authors have read and agreed to the published version of the manuscript.

Funding

This study was funded by the Project "Dunărea la Raport", contract number 79/28.01.2022 between GWP-Romania and "Mai Mult Verde" NGO associations, within the framework of „Cu Apele Curate"/ "Clean Waters" programme, supported by Lidl Romania. This study was supported by the REXDAN research infrastructure created within the project "An integrated system of research and monitoring of the complex environment in the area of the Danube River", code SMIS 127065, co-financed by the European Regional Development Fund through the Competitiveness Operational Program 2014–2020, contract no. 309/10.07.2021.

Availability of data and materials

All data generated or analyzed during this study are included in this published article [and its supplementary information files].

Declarations

Ethics approval and consent to participate

Not applicable.

Consent for publication

Not applicable.

Competing interests

The authors declare that they have no known competing financial interests in personal relationships that could have could have appeared to influence the work reported in this paper.

Author details

[1]Laboratory of Nanochemistry/Centre of Nanostructures and Functional Materials/LNC-CNMF, "Dunărea de Jos" University of Galați, 111 Domnească Street, 800201 Galați, Romania. [2]REXDAN Research Infrastructure of "Dunarea de Jos" University of Galati, Str. George Cosbuc, 98, 800385 Galati, Romania. [3]Institute of Hydraulic Engineering and River Research, Department of Water, Atmosphere and Environment, University of Natural Resources and Life Sciences, Vienna, Am Brigittenauer Sporn 3, 1200 Vienna, Austria. [4]National Institute of Hydrology and Water Management, Sos. Bucuresti-Ploiesti, no. 97, 01686 Bucharest, Romania. [5]Cross-Border Faculty, "Dunarea de Jos" University of Galati, 111 Domneasca Str., 800201 Galati, Romania. [6]Center of Excellence Polymer Processing, "Dunarea de Jos" University of Galati, 47 Domneasca, 800008 Galati, Romania. [7]Department of Chemistry, Physics and Environment, "Dunarea de Jos" University of Galati, 800008 Galati, Romania. [8]Global Water

Partnership Romania/Asociația Parteneriatul Global al Apei din România GWP ROMÂNIA, Roșiori 4, Tg. Bujor, Galați, Romania.

Received: 30 March 2024 Accepted: 30 July 2024
Published online: 01 September 2024

References

1. Roebroek CTJ, Laufkötter C, González-Fernández D, van Emmerik T (2022) The quest for the missing plastics: large uncertainties in river plastic export into the sea. Environ Pollut. https://doi.org/10.1016/j.envpol.2022.119948
2. Lebreton L, Andrady A (2019) Future scenarios of global plastic waste generation and disposal. Palgrave Commun 5:1–11. https://doi.org/10.1057/s41599-018-0212-7
3. Galgani F, Brien AS, Weis J, Ioakeimidis C, Schuyler Q, Makarenko I, Griffiths H, Bondareff J, Vethaak D, Deidun A et al (2021) Are litter, plastic and microplastic quantities increasing in the ocean? Microplast Nanoplast 1:8–11. https://doi.org/10.1186/s43591-020-00002-8
4. Schmid C, Cozzarini L, Zambello E (2021) Microplastic's story. Mar Pollut Bull 162:111820. https://doi.org/10.1016/j.marpolbul.2020.111820
5. Lau WWY, Shiran Y, Bailey RM, Cook E, Stuchtey MR, Koskella J, Velis CA, Godfrey L, Boucher J, Murphy MB et al (2020) Evaluating scenarios toward zero plastic pollution. Science (1979). https://doi.org/10.1126/SCIENCE.ABA9475
6. Lu HC, Ziajahromi S, Neale PA, Leusch FDL (2021) A systematic review of freshwater microplastics in water and sediments: recommendations for harmonisation to enhance future study comparisons. Sci Total Environ 781:146693. https://doi.org/10.1016/j.scitotenv.2021.146693
7. Li Y, Lu Z, Zheng H, Wang J, Chen C (2020) Microplastics in surface water and sediments of chongming island in the Yangtze Estuary, China. Environ Sci Eur. https://doi.org/10.1186/s12302-020-0297-7
8. Botterell ZLR, Beaumont N, Dorrington T, Steinke M, Thompson RC, Lindeque PK (2019) Bioavailability and effects of microplastics on marine zooplankton: a review. Environ Pollut 245:98–110. https://doi.org/10.1016/j.envpol.2018.10.065
9. D'Hont A, Gittenberger A, Leuven RSEW, Hendriks AJ (2021) Dropping the microbead: source and sink related microplastic distribution in the black sea and caspian sea basins. Mar Pollut Bull 173:112982. https://doi.org/10.1016/j.marpolbul.2021.112982
10. Hohenblum P, Frischenschlager H, Reisinger H, Konecny R, Uhl M, Mühlegger S, Hohenblum P, Habersack H, Marcel Liedermann PG, Frischenschlager H, Weidenhiller B et al (2015) Plastik in Der Donau. ISBN 9783990043585. https://www.umweltbundesamt.at/fileadmin/site/publikationen/rep0547.pdf
11. Lai H, Liu X, Qu M (2022) Nanoplastics and human health: hazard identification and biointerface. Nanomaterials. https://doi.org/10.3390/nano12081298
12. Jacques O, Prosser RS (2021) A probabilistic risk assessment of microplastics in soil ecosystems. Sci Total Environ 757:143987. https://doi.org/10.1016/j.scitotenv.2020.143987
13. Braun U, Kittner M, Kerndorff A, Ricking M, Bednarz M, Obermaier N, Lukas M, Asenova M, Bordós G, Eisentraut P et al (2022) Microplastics in the Danube river basin: a first comprehensive screening with a harmonized analytical approach. ACS ES T Water 2:1174–1181. https://doi.org/10.1021/acsestwater.1c00439
14. Stark M (2019) Marine anthropogenic litter. Springer, Cham
15. Hwang J, Choi D, Han S, Jung SY, Choi J, Hong J (2020) Potential toxicity of polystyrene microplastic particles. Sci Rep 10:1–12. https://doi.org/10.1038/s41598-020-64464-9
16. Ragusa A, Svelato A, Santacroce C, Catalano P, Notarstefano V, Carnevali O, Papa F, Rongioletti MCA, Baiocco F, Draghi S et al (2021) Plasticenta: first evidence of microplastics in human placenta. Environ Int 146:106274. https://doi.org/10.1016/j.envint.2020.106274
17. Kenyon KW, E.K. (1969) Laysan albatrosses swallow indigestible matter. Auk 86(2):339–343
18. Merrell TR (1980) Accumulation of plastic litter on beaches of Amchitka Island, Alaska. Mar Environ Res 3:171–184. https://doi.org/10.1016/0141-1136(80)90025-2
19. Xiang Y, Jiang L, Zhou Y, Luo Z, Zhi D, Yang J, Lam SS (2021) Microplastics and environmental pollutants: key interaction and toxicology in aquatic and soil environments. J Hazard Mater 422:126843. https://doi.org/10.1016/j.jhazmat.2021.126843
20. Park EJ, Han JS, Park EJ, Seong E, Lee GH, Kim DW, Son HY, Han HY, Lee BS (2020) Repeated-oral dose toxicity of polyethylene microplastics and the possible implications on reproduction and development of the next generation. Toxicol Lett 324:75–85. https://doi.org/10.1016/j.toxlet.2020.01.008
21. Hamidian AH, Ozumchelouei EJ, Feizi F, Wu C, Zhang Y, Yang M (2021) A review on the characteristics of microplastics in wastewater treatment plants: a source for toxic chemicals. J Clean Prod 295:126480. https://doi.org/10.1016/j.jclepro.2021.126480
22. Nayebi B, Khurana P, Pulicharla R, Karimpour S, Brar SK (2023) Preservation, storage, and sample preparation methods for freshwater microplastics - a comprehensive review. Environ Sci Adv 2:1060–1081. https://doi.org/10.1039/d3va00043e
23. Schrank I, Löder MGJ, Imhof HK, Moses SR, Heß M, Schwaiger J, Laforsch C (2022) Riverine microplastic contamination in southwest Germany: a large-scale survey. Front Earth Sci (Lausanne) 10:1–17. https://doi.org/10.3389/feart.2022.794250
24. Lebreton LCM, Van Der Zwet J, Damsteeg JW, Slat B, Andrady A, Reisser J (2017) River plastic emissions to the world's oceans. Nat Commun 8:1–10. https://doi.org/10.1038/ncomms15611
25. Benedikt M, McCaffrey S (2006) The Danube River Basin - Facts and Figures. The Multi-Governance of Water: Four Case Studies. 79–101. https://www.icpdr.org/sites/default/files/nodes/documents/icpdr_facts_figures.pdf
26. Lechner A, Keckeis H, Lumesberger-Loisl F, Zens B, Krusch R, Tritthart M, Glas M, Schludermann E (2014) The Danube so colourful: a potpourri of plastic litter outnumbers fish larvae in Europe's second largest river. Environ Pollut 188:177–181. https://doi.org/10.1016/j.envpol.2014.02.006
27. Pojar I, Dobre O, Lazăr C, Baboș T, Ristea O, Constantin A, Cristoiu N (2024) Microplastic Evaluation in Water and Sediments of a Dam Reservoir–Riverine System in the Eastern Carpathians, Romania. Sustainability (Switzerland). p. 16 https://doi.org/10.3390/su16114541
28. Kittlaus S, Kardos MK, Dudás KM, Weber N, Clement A, Petkova S, Sukovic D, Kučić Grgić D, Kovacs A, Kocman D et al (2024) A harmonized danube basin-wide multi-compartment concentration database to support inventories of micropollutant emissions to surface waters. Environ Sci Eur. https://doi.org/10.1186/s12302-024-00862-4
29. Strokal V, Kuiper EJ, Bak MP, Vriend P, Wang M, van Wijnen J, Strokal M (2022) Future microplastics in the black sea: river exports and reduction options for zero pollution. Mar Pollut Bull 178:113633. https://doi.org/10.1016/j.marpolbul.2022.113633
30. Kiefer T, Knoll M, Fath A (2023) Comparing methods for microplastic quantification using the Danube as a model. Microplastics 2:322–333. https://doi.org/10.3390/microplastics2040025
31. Pojar I, Tiron Duțu L, Pop CI, Duțu F (2021) Hydrodynamic observations on microplastic abundances and morphologies in the Danube delta, Romania. AgroLife Sci J 10:142–149. https://doi.org/10.17930/AGL2021218
32. Pojar I, Kochleus C, Dierkes G, Ehlers SM, Reifferscheid G, Stock F (2021) Quantitative and qualitative evaluation of plastic particles in surface waters of the western black sea. Environ Pollut 268:115724. https://doi.org/10.1016/j.envpol.2020.115724
33. Pojar I, Stănică A, Stock F, Kochleus C, Schultz M, Bradley C (2021) Sedimentary microplastic concentrations from the Romanian Danube river to the black sea. Sci Rep 11:1–10. https://doi.org/10.1038/s41598-021-81724-4
34. Liedermann M, Gmeiner P, Pessenlehner S, Haimann M, Hohenblum P, Habersack H (2018) A methodology for measuring microplastic transport in large or medium rivers. Water 10:1–12. https://doi.org/10.3390/w10040414
35. van Emmerik T, Schwarz A (2020) Plastic debris in rivers. Wiley Interdiscip Rev Water 7:1–24. https://doi.org/10.1002/wat2.1398
36. Georgescu PL, Moldovanu S, Iticescu C, Calmuc M, Calmuc V, Topa C, Moraru L (2023) Assessing and forecasting water quality in the danube river by using neural network approaches. Sci Total Environ 879:162998. https://doi.org/10.1016/j.scitotenv.2023.162998

37. Haimann M, Liedermann M, Lalk P, Habersack H (2014) An integrated suspended sediment transport monitoring and analysis concept. Int J Sedim Res 29:135–148. https://doi.org/10.1016/S1001-6279(14)60030-5
38. Li J, Liu H, Paul Chen J (2018) Microplastics in freshwater systems: a review on occurrence, environmental effects, and methods for microplastics detection. Water Res 137:362–374. https://doi.org/10.1016/j.watres.2017.12.056
39. Strokal M, Vriend P, Wijnen VJ, Kroeze C, van Emmerik T (2021) The MARINA-Plastic Model: Global River Export of Macro- and Microplastics from over 10,000 Sub-Basins to Coastal Seas. EGU General Assembly 2021, online, 19–30 Apr 2021, EGU21-649. 10.5194/egusphere-egu21-649
40. Scherer C, Weber A, Stock F, Vurusic S, Egerci H, Kochleus C, Arendt N, Foeldi C, Dierkes G, Wagner M et al (2020) Comparative assessment of microplastics in water and sediment of a large European river. Sci Total Environ 738:139866. https://doi.org/10.1016/J.SCITOTENV.2020.139866
41. Mitra S, Jørgensen M, Pedersen WA, Almdal K, Banerjee D (2009) Structural determination of Ethylene-Propylene-Diene Rubber (EPDM) containing high degree of controlled long-chain branching. J Appl Polym Sci 116:2962–2972. https://doi.org/10.1002/app
42. Wang G, Lu J, Li W, Ning J, Zhou L, Tong Y, Liu Z, Zhou H, Xiayihazi N (2021) Seasonal variation and risk assessment of microplastics in surface water of the Manas river basin. China Ecotoxicol Environ Saf 208:111477. https://doi.org/10.1016/j.ecoenv.2020.111477
43. Literáthy P, László F (1999) Micropollutants in the Danube river basin. Water Sci Technol 40:17–26. https://doi.org/10.1016/S0273-1223(99)00668-X
44. Horton AA, Dixon SJ (2018) Microplastics: an introduction to environmental transport processes. Wiley Interdiscip Rev Water 5:1–10. https://doi.org/10.1002/WAT2.1268
45. Skalska K, Ockelford A, Ebdon JE, Cundy AB (2020) Riverine microplastics: behaviour, spatio-temporal variability, and recommendations for standardised sampling and monitoring. J Water Process Eng 38:101600. https://doi.org/10.1016/j.jwpe.2020.101600
46. Sutkar PR, Gadewar RD, Dhulap VP (2023) Recent trends in degradation of microplastics in the environment: a state-of-the-art review. J Hazard Mater Adv 11:100343. https://doi.org/10.1016/j.hazadv.2023.100343
47. Kumar R, Sharma P, Verma A, Jha PK, Singh P, Gupta PK, Chandra R, Vara Prasad PV (2021) Effect of physical characteristics and hydrodynamic conditions on transport and deposition of microplastics in riverine ecosystem. Water. https://doi.org/10.3390/w13192710
48. Range D, Scherer C, Stock F, Ternes TA, Hoffmann TO (2023) Hydrogeomorphic perspectives on microplastic distribution in freshwater river systems: a critical review. Water Res 245:120567. https://doi.org/10.1016/j.watres.2023.120567
49. Strokal M, Vriend P, Bak MP, Kroeze C, van Wijnen J, van Emmerik T (2023) River export of macro- and microplastics to seas by sources worldwide. Nat Commun. https://doi.org/10.1038/s41467-023-40501-9
50. Brandon J, Goldstein M, Ohman MD (2016) Long-term aging and degradation of microplastic particles: comparing in situ oceanic and experimental weathering patterns. Mar Pollut Bull 110:299–308. https://doi.org/10.1016/j.marpolbul.2016.06.048
51. Padervand M, Lichtfouse E, Robert D, Wang C (2020) Removal of microplastics from the environment. A review. Environ Chem Lett 18:807–828. https://doi.org/10.1007/s10311-020-00983-1
52. Carson HS, Nerheim MS, Carroll KA, Eriksen M (2013) The plastic-associated microorganisms of the North Pacific Gyre. Mar Pollut Bull 75:126–132. https://doi.org/10.1016/j.marpolbul.2013.07.054
53. Cooper DA, Corcoran PL (2010) Effects of mechanical and chemical processes on the degradation of plastic beach debris on the Island of Kauai, Hawaii. Mar Pollut Bull 60:650–654. https://doi.org/10.1016/j.marpolbul.2009.12.026

Publisher's Note